American Journal of Mechanical Engineering, 2019, Vol. 7, No. 1, 1-8
Available online at http://pubs.sciepub.com/ajme/7/1/1
Published by Science and Education Publishing
DOI:10.12691/ajme-7-1-1

Review on Simulation of Non-reacting Fuel Spray

Hashem Nowruzi*

Maritime Engineering Department, Amirkabir University of Technology, Tehran, Iran
*Corresponding author: h.nowruzi@aut.ac.ir

Received September 08, 2018; Revised October 19, 2018; Accepted January 16, 2019

Abstract Marine diesel engines (MDEs) are interested due to their ability to generate high power and fuel economy. Nowadays, researchers are seeking different methods to develop the performance of MDEs. Fuels spray behavior has key role to improve of MDEs. Therefore, in the present paper, fundamental of non-reacting and non-evaporating fuel spray simulation are reviewed. For this purpose, recent works in this context are presented and after that, microscopic and macroscopic characteristics of non-reacting spray are described. Finally, the basic formulations of Eulerian-Lagrangian multiphase and different breakup models are presented.

Keywords: *non-reacting spray, CFD, fuel, marine diesel engines, breakup model*

Cite This Article: Hashem Nowruzi, "Review on Simulation of Non-reacting Fuel Spray." *American Journal of Mechanical Engineering*, vol. 7, no. 1 (2017): 1-8. doi: 10.12691/ajme-7-1-1.

1. Introduction

Internal combustion engines (ICEs) are the main engines in different industries, i.e., maritime, railway, power plant. Main reason for attention to ICEs is depended on their capability to generate high power associated with fuel economy. In example, nowadays, a large number of ships engine have large marine diesel engines due to their proper performance and an appropriate lifetime. Future perspective of ICEs and especially marine diesel engines (MDEs) is dependent to enhancement of their performance and diminish of their pollutions. For this purpose, various solutions such as using bio-fuels, different injection methods (e.g. direct injection) and improve of ambient condition (e.g. backpressure and ambient temperature) are suggested. So, various researches are done to show the effects of bio-fuels and alcohols based fuel [1-15], injection methods and ambient condition [16-25] on the behavior of fuel spray as main affective parameter on the non-reacting performance in MDEs. For example, Nowruzi et al. [1] shows that the one of the solutions to increase the quality of Heavy fuel (HF) and reduce of their emissions is addition of alcohols including ethanol, methanol, and butanol to the reference fuels. They found the higher comparative advantage of butanol relative to ethanol and methanol in combination with diesel fuels [2]. Miers et al. [3] investigated the effects of blending 20% and 40% by volume of butanol with ultra-low-sulfur diesel fuel on efficiency and pollution of a Mercedes-Benz C220 turbo diesel vehicle. Rakopoulos et al. [4] studied the influences of using ethanol or n-butanol diesel fuel blend on diesel engine emission. They indicated that, 5% and 10% of ethanol blended with diesel fuel resulted to decrease of smoke density. Other experimental studies on alcohol based fuels are conducted by Rakopoulos et al. [5,6]. Dogan et al. [7] studied the impression of alternative fuels on smoke, CO and NOx. They indicated that using alcohol based fuels will be resulted to decrease of CO and NOx. Zhang et al. [8] also investigated a major reduction of PM by using 5%, 10%, 15% and 20% of butanol blend with ultra low sulfur diesel in a non-road diesel engine. In addition, the combustion effects of blend of 80% butanol with 20% low sulfur diesel at two stroke single cylinder is studied by Tornatore et al. [9]. Biao et al. [10] showed that 30% butanol-diesel fuels significantly reduce the soot emission in high speed heavy duty diesel engine. Adding water into combustion chamber is another strategy for emission control with respect to low-temperature diesel combustion (LTC) technique by impression on high temperature zone (See Figure 1) [11]. Recently, the effects of different bio-fuel such as micro-algae and alcohol based fuels on non-reacting spray are also studied by Nowruzi el al. [12,13,14,15].

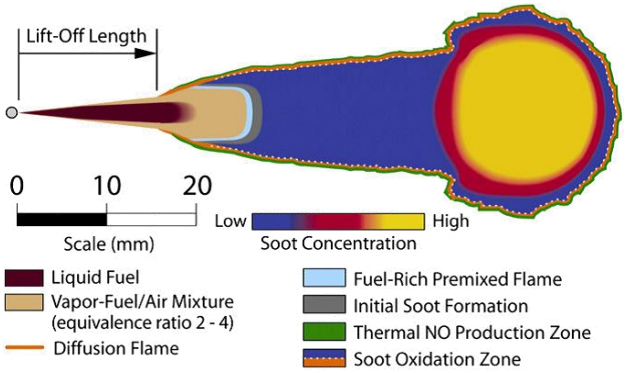

Figure 1. High temperature zone formation in injection of fuel [11]

On the other hands, a comprehensive study related to study of spray behavior under different injection and conditions are done by researchers. It's notable that, improve of spray under non-reacting condition is easier and more operational with lower computational cost compared to the reacting conditions. Injection pressure is

one of the most important parameter. Level of atomization will be increased by an enhancement of injection pressure. As a result, upper level of atomization will be cause to formation of further homogeneous mixture [16,17,18,19].

Nishida et al. [20] experimentally studied the effects of high and ultra-high injection pressures of 100, 200, and 300 MPa on the spray penetration and sauter mean diameter (SMD) for diesel fuel. Non-evaporating properties of bio-diesels and diesel at ultra-high injection pressures of 100, upto 300 MPa are investigated by Wang et al. [21]. Spray-induced air flow under high injection pressure up to 300MPa is evaluated by Ghasemi et al. [22]. Moreover, Fink et al. [23] evaluated the HFO, diesel fuel, and fuel-water emulsion on spray characteristics, experimentally. In this research, three injection pressures of 60, 100 and 140 MPa are considered. They indicated that the spray tip penetration for HFO is approximately similar to diesel fuel, while, spray cone angle and spray volume are decreased in case of HFO. Fluid flow of liquid swirl from injector at different range of chamber backpressures is numerically studied by Chen et al. [24]. Park et al.[25] showed that by enhancement of ambient gas temperature to the boiling point, SMD will be increased. Roisman et al. [26] proposed a predictive equation to determine spray tip penetration based on experimental study.

Recently, Yousefifard et al. [27,28] studied the effects of different ambient pressure and temperatures on the on-reacting spray behavior by CFD simulation via open source software of OpenFOAM. Nowadays, artificial neural networks are also presented to prediction of physical phenomenon by reference numerical and experimental data [29,30,31]. In example, Nowruzi et al. [32] Prediction of impinging sprays penetration and cone angle under different injection and ambient conditions by means of CFD and ANNs.

Based on cited works, one can be concluded the significant role of physical parameters such as injected fuels, ambient temperature, and ambient backpressure and injection characteristics on the spray behavior. Consequently, importance of non-reacting spray simulation to investigate the effects of fuel spray on the efficiency and emission of ICEs is obvious. Therefore, the microscopic and macroscopic characteristics of non-reacting spray are described in following sections and after that the basic formulations of Eulerian-Lagrangian multiphase are presented.

2. Macroscopic and Microscopic Characteristics of Fuel Spray

Different macroscopic and microscopic characteristics of fuel spray are effective on atomization, breakup procedure and on the level of air-fuel mixture as significant effective parameter on engine efficiency before the combustion procedure. So, well-know investigation on non-reacting fuel spray (i.e., liquid spray) behavior by study of macroscopic and microscopic characteristics is necessary

2.1. Liquid Spray

Two major regions of liquid and gaseous are visible for injected fuel spray in the combustion chamber. Under non-reacting condition, liquid zone is detectable. Schematic of liquid structure of fuel spray during breakup procedure is illustrated in Figure 2.

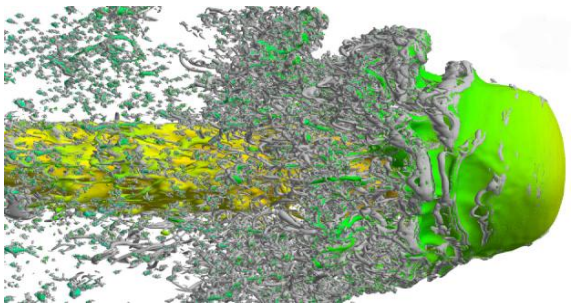

Figure 2. Schematic of breakup of liquid fuel spray [33]

Figure 3 is presented for detail investigation on liquid spray region of injected fuel spray. As may be seen in Figure 3, injected fuel spray is divided into three major zones liquid core, dispersed region and evaporated region. Remarkable breakup of the liquid fuel will be occur nearby the hole injector in the liquid core region. Moreover, gas penetration into the injection area for generation of air-fuel mixture is visible in the dispersed region. In this region, fuel particles are also broken to smaller sizes. After that, vaporization of fuel under ignition procedure will be start in the evaporated region. In the current study, we focused on liquid core region [34].

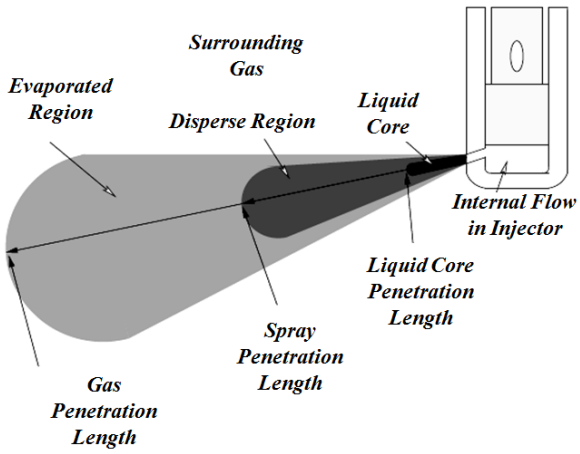

Figure 3. Different zones of spray under non-reacting condition [34]

Figure 4 is presented to show the different regions in the liquid spray. Liquid spray will be injected into the gaseous environment by injection velocity. Gaseous medium is a composition of air and hot gases (from combustion or recirculation gas). As may be seen in Fig.4, atomization region is the first region after the nozzle. Liquid fuel core decomposition into the blobs, ligaments and droplets is visible in this region. Blobs are capable to become ligaments and ligaments are also able to breakup into droplets. Primary breakup is the procedure of liquid fuel transition in the atomization region. Usually, primary breakup will be neglected due to high pressure and some uncertainty in this region. Under this condition, injected droplets intended for secondary breakup [1,18,34]. In dense spray (second zone in Figure 4) is the region where secondary breakup will be occurring for drops and ligaments. According to aerodynamic interaction of gaseous medium and fuel droplets, numerous ligaments

are detectable in this region. Third region is spray region where numerous spherical droplets will be formed in this region. Different parameters of injector size, thermophysical characteristics of fuel and physical parameters of combustion chamber (i.e., backpressure) are impressive on behavior of liquid spray [35].

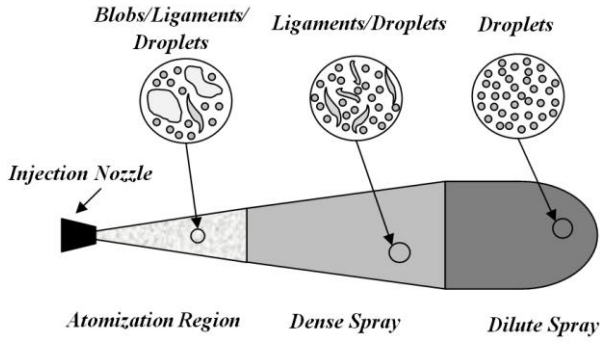

Figure 4. Schematic of liquid spray [1]

2.2. Liquid Spray Characteristics

Four different microscopic and macroscopic characteristics will be evaluated for investigation of non-reacting fuel spray. Three macroscopic properties are liquid spray penetration length, spray cone angle and spray volume. Moreover, microscopic characteristics of sauter mean diameter (SMD) will be used for evaluation of breakup procedure.

Macroscopic criteria of penetration length are the length of the continuous liquid phase. For this purpose, as may be seen in Figure 5, we measure the axial distance of fuel from the injector up to the farthest axial location (ratio of air-fuel volume lower than 0.1%). Moreover, angle among the two lines from the injector's nozzle to the two points of maxima radial distance of the liquid parcels will be used for determination of spray cone angle (See Figure 5).

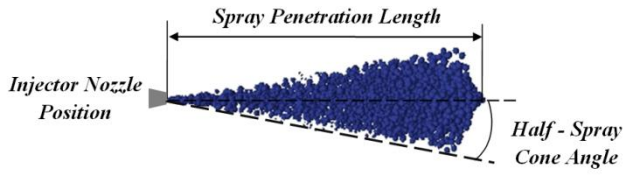

Figure 5. Spray penetration length and half spray cone angle [1,34]

On the other hand, to more detail investigation on air-fuel mixture, volume of fuel spray will be evaluated. The exact value of liquid volume is not feasible in experiment [36], while, in CFD analysis, spray volume based on spray penetration length and cone angle, has following form:

$$V(t)=\frac{1}{3}\pi S^3(t)\tan^2\left(\frac{\theta}{2}\right)\frac{\left(1+2\tan\left(\frac{\theta}{2}\right)\right)}{\left(1+\tan\left(\frac{\theta}{2}\right)\right)^3} \quad (1)$$

here, the cone angle is shown by θ and spray penetration length is presented by S. Microscopic characteristics of SMD is the average diameter of all droplets. Continued, CFD simulation of non-Reacting spray and mathematical formulation of primary and secondary breakup are presented and discussed.

3. Mathematical Modeling and Numerical Procedure

Phenomenon of fuel spray and its breakup have two-phase regime. In the current section, we described the physic of the problem and governing equation related to injected fuel behavior and the breakup procedure. Eulerian–Lagrangian multiphase scheme is the selected approach to solve of two-phase flow of injected fuel [12,13,14,15,16]. In this approach, continuous fuel flow will be simulated by Navier-Stokes equations, while, fuel particles are modeled via Lagrangian scheme and based on the Newton's laws of motion. The interactions of these two schemes are considered as source term on the governing equations. So that, impression of discrete phase of fuel will be intended as source term in the conservation equation of gaseous medium, while, the effects of gaseous phase on the dispersion of the liquid fuel will be applied via local value of gaseous temperature and velocity at the grid cell, where liquid droplets are passing inside them under each time step [34].

In Eulerian–Lagrangian multiphase scheme, we considered five equations such as conservation of mass, energy, and the components of the momentum. Turbulence modeling is also applied by Reynolds averaged Navier Stokes simulation (RANS). Lagrangian particle tracking (LPT) method is another approach that is useful to model of discrete phase of the fuels. As stated before, breakup and mass and heat transfer will be applied as source term in the equations to make a relation between the Eulerian scheme and Lagrangian approach.

Four different regimes are observable for liquid spray. Rayleigh assumption, primary wave, secondary wave and very small particle are these four regimes, which are depended on SMD and three non-dimensional numbers of Reynolds, Weber and Ohnesorge number as follows:

$$\mathrm{Re}_l=\frac{du_r}{\upsilon_l} \quad (2)$$

$$We_g=\frac{\rho_g u_r^2 d}{\sigma} \quad (3)$$

$$We_l=\frac{\rho_l u_r^2 d}{\sigma} \quad (4)$$

$$Oh=\frac{\mu_l}{\sqrt{\rho_l\sigma d}}=\frac{We_l}{\mathrm{Re}_l} \quad (5)$$

where, hole diameter is shown by d and relative velocity between the fuel and air is u_r. Moreover, kinematic viscosity and surface tension are presented by υ_l and σ. Also, liquid fuel and gaseous phase are indexed by the subscript of l and g, respectively. Two others parameter to investigate of fuel particle are volume fraction of particle per fluid and Stokes number. Volume fraction of particle per fluid has following form:

$$c = \frac{V_p}{V_f} \tag{6}$$

where, V_p and V_f are volume fraction of particle and fluid, respectively. In addition, Stokes number can be express as follows:

$$St = \frac{\tau_p}{\tau_f} \tag{7}$$

here, momentum relaxation time is shown by τ_p as follows:

$$\tau_p = \frac{\rho_p d^2}{18\rho_g \upsilon} \tag{8}$$

where, particle diameter is shown by d and in case of $St \gg 1$ turbulence will be amplified, however, in case of $St \ll 1$, damping of turbulence is visible.

3.1. Continuous Phase Modeling

Continuous phase of fluid will be modeled by conservative equations of mass, momentum and energy [37,38] as follows:

$$\frac{\partial \rho}{\partial t} + \frac{\partial}{\partial x_j}\left(\rho u_j\right) = 0 \tag{9}$$

here, fluid density is ρ and jth fluid velocity component is shown by u_j. In this condition, momentum equation has following form:

$$\frac{\partial}{\partial t}\left(\rho u_i\right) + \frac{\partial}{\partial x_j}\left(\rho u_j u_i\right) = \rho g_i - \frac{\partial p}{\partial x_i} + \frac{\partial \tau_{ij}}{\partial x_j} \tag{10}$$

where, pressure and stress tensor are p and τ_{ij}, respectively. Based on the first law of thermodynamic, conservation equations of energy can be expressed as:

$$\frac{\partial \rho E}{\partial t} + \frac{\partial\left(\rho E u_i\right)}{\partial x_i} = -\frac{\partial q_j}{\partial x_j} + \rho g_i u_i - \frac{\partial}{\partial x_j}\left(p u_j\right) + \frac{\partial}{\partial x_i}\left(\tau_{ij} u_j\right) \tag{11}$$

here, total energy per volume unite and i th vector of energy flow are shown by E and q_i. For turbulence modeling, averaged of Navier-Stokes equations can be used as follows:

$$\frac{\partial \rho}{\partial t} + \frac{\partial}{\partial x_j}\left(\rho u_j\right) = 0 \tag{12}$$

$$\frac{\partial}{\partial t}\left(\rho u_i\right) + \frac{\partial}{\partial x_j}\left(\rho u_j u_i\right) = -\frac{\partial P}{\partial x_i} + \frac{\partial}{\partial x_j}\left(\tau_{ij} + \tau_{ij}^R\right) \tag{13}$$

where, Favre averaging of velocity is $u_i = \tilde{u}_i^o$. Moreover, $\tau_{ij} = \bar{\tau}_{ij}^o$ as Reynolds averaging variables is:

$$\tau_{ij}^R = -\rho \tilde{u}_i' \tilde{u}_j' \tag{14}$$

Reynolds tensor stress determines impression of turbulence oscillation. To solve of unknowns equations, different models in RANS are suggested. One of an efficient model is $k-\varepsilon$ [39]. In this model, kinematic energy (Eq.15) and energy dissipation (Eq.16) are as follows:

$$k = \frac{1}{2}\left\|u'\right\|^2 \tag{15}$$

$$\varepsilon = 2\upsilon \tilde{S}_{ij} \tilde{S}_{ij}. \tag{16}$$

Now, variables of k and ε are as follows:

$$\frac{\partial \rho k}{\partial t} + \frac{\partial \rho k u_i}{\partial x_i} = \frac{\partial}{\partial x_j}\left[\left(\alpha_k \mu + \mu_t\right)\frac{\partial k}{\partial x_j}\right] + P_k - \frac{2}{3}\rho k \frac{\partial u_k}{\partial x_k} - \rho\varepsilon \tag{17}$$

$$\frac{\partial \rho \varepsilon}{\partial t} + \frac{\partial \rho \varepsilon u_i}{\partial x_i} = \frac{\partial}{\partial x_j}\left[\left(\alpha_\varepsilon \mu + \mu_t\right)\frac{\partial \varepsilon}{\partial x_j}\right] + C_1 P_k \frac{\varepsilon}{k} - \left(\frac{2}{3}C_1 + C_3\right)\rho\varepsilon \frac{\partial u_k}{\partial x_k} - C_2 \rho \frac{\varepsilon^2}{k} \tag{18}$$

where, C1=1.44, C2=1.92, C3=-0.33, αk=1, αϵ=0.76923 and $P_k = \mu_t |S|^2$ and $|S| \equiv \sqrt{2S_{ij}S_{ij}}$ [39]. Another turbulence model that is efficient for non-reacting fuel spray is large eddy simulation (LES) [17]. In this mode, sub-grid stress tensor τ_{ij}^{sgs} is:

$$\tau_{ij}^{sgs} = \frac{2}{3}k^{sgs}\delta_{ij} - 2\upsilon_t\left(\bar{S}_{ij} - \frac{1}{3}\bar{S}_{kk}\delta_{ij}\right) \tag{19}$$

here, turbulent kinematic viscosity is presented by $\upsilon_t = C_k \bar{\Delta}\sqrt{k^{sgs}}$, where, characteristic grid length is $\bar{\Delta}$ and sub-grid scale kinetic energy is k^{sgs}. In Continuous phase modeling, combined scheme of SIMPLE (semi-implicit method for pressure-linked equations) and PISO (pressure implicit with splitting of operator) will be utilized for couple of velocity-pressure [40].

3.2. Dispersed Fluid Simulation

Main purpose of dispersed fluid modeling is determination of location, diameter, temperature and velocity of particles. Lagrangian particle tracking (LPT) approach is used to determine the rate of rotation of particles [35]. To this accomplishment, stochastically spray is shown in Eq.(20), where impression of collision of the droplets and breakup procedure is presented by source term as follows:

$$\frac{\partial f}{\partial t} + \nabla_x.(fV) + \nabla_v.(fF) + \frac{\partial}{\partial r}(fR) + \frac{\partial}{\partial T_d}\left(f\dot{T}_d\right) + \frac{\partial}{\partial y}(f\dot{y}) + \frac{\partial}{\partial \dot{y}}(f\ddot{y}) = \dot{f}_{coll}\ \dot{f}_{bu} \tag{20}$$

where, probable number of droplets per unit volume at position of x, time t and radius from r to r+dr, temperature form T to T+dT and velocity change from u into the u+du

and according to distortion of y into the y+dy up to $\dot{y}+d\dot{y}$ is determined by $f(X,V,r,T_d,T,y,\dot{y},t)dVdrdT_d dydy$. In this condition, acting force on the fuel droplet is:

$$\frac{1}{6}\rho_p \pi d^3 \frac{du_p}{dt} = \frac{1}{2}\left(u_g - u_p\right)\left|u_g - u_p\right|\rho_g C_D \frac{\pi d^2}{4} \quad (21)$$

where, particle velocity is u_p, and gas velocity is shown by u_g. Droplet drag coefficient is also presented by C_D as follows:

$$C_D = \begin{cases} \frac{24}{\mathrm{Re}_p}\left(1+\frac{1}{6}\mathrm{Re}_p^{2/3}\right), & \mathrm{Re}_p < 1000 \\ 0.424, & \mathrm{Re}_p \geq 1000. \end{cases} \quad (22)$$

In Eq. (22), droplet Reynolds number is defined by $\mathrm{Re}_p = \left|u_g - u_p\right| d / \upsilon_g$. Up to now, different breakup model are suggested by scholars that the more efficient model are presented.

3.3. Breakup Procedure

Simulation of primary and secondary breakups is an important step in non-reacting spray modeling. Investigation of primary breakup is complicated due to ultra high pressure of liquid fuel near the nozzle of injector. Therefore, initial radius of the fuel droplets and spray angle will be used as initial condition of secondary breakup. Blob method is the interested approach to primary breakup that is suggested by Reitz and Diwakar [41,42] as may be seen in Figure 6. In this method, atomization is assumed for droplets breakup and large droplets are considered for secondary breakup.

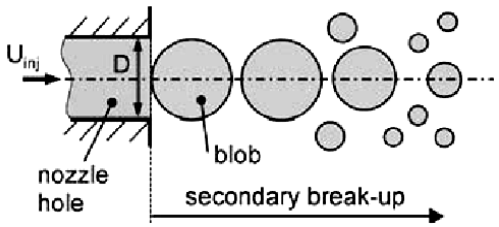

Figure 6. Schematic of Blob method [41,42]

Secondary breakup is the main step in numerical simulation of high injection pressure non-reacting spray. In secondary breakup, velocity among the fuel droplets and ambient gas (i.e., u_{rel}) is the reason of breakup due to aerodynamic force. Aerodynamic force will be resulted to amplify of instabilities on the fuel surface and surface tension overcomes the deformation forces. Ratio between the aerodynamic force and surface tension is defined by Weber number. Different secondary breakup models are presented. Among them, RD model as combination of Bag breakup and stripping breakup (See Figure 7) is one of the interested model that presented by Reitz and Diwakar [41,42]. In this model, Bag Breakup is visible in case of:

$$We_g = \frac{\rho_g u_{rel}^2 D_d}{\sigma} > 12 \quad (23)$$

And stripping breakup is happen in the condition of:

$$\frac{We_g}{\sqrt{\mathrm{Re}}} > 0.5 \quad (24)$$

here, Reynolds number and gas kinematic viscosity is shown by $\mathrm{Re} = u_{rel} D_d / \nu_g$ and ν_g, respectively.

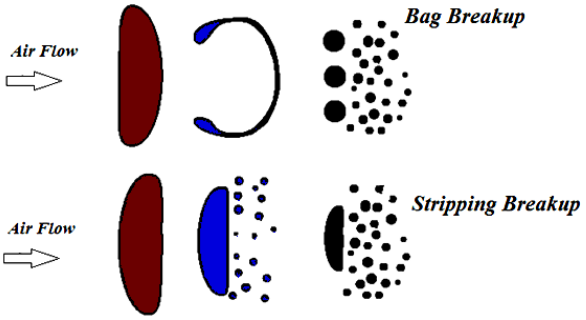

Figure 7. Schematic of bag breakup and stripping breakup in RD model [34]

Another secondary breakup model is wave model (Kelvin–Helmholtz (KH)) that presented by Reitz [43]. In this model, instability will be growth on the liquid jet surface via radius of r_0 and the main assumption is the spectrum of sinusoidal wave on the surface on liquid fuel that is formed by aerodynamic force. In this model, wavelength and growth rate of instability wave are Ω_{KH} and Λ_{KH} that are as follows:

$$\Omega_{KH}\left[\frac{\rho_l r_0^3}{\sigma}\right]^{0.5} = \frac{0.34+0.38\cdot We_g^{1.5}}{(1+Oh)(1+1.4\cdot T^{0.6})} \quad (25)$$

$$\frac{\Lambda_{KH}}{r_0} = 9.02\frac{(1+0.45\cdot Oh^{0.5})(1+0.4\cdot T^{0.7})}{(1+0.865\cdot We_g^{1.67})^{0.6}} \quad (26)$$

here,

$$\begin{cases} T = Oh\sqrt{We_g} \\ We_g = \frac{\rho_g u_{rel}^2 r_0}{\sigma} \\ We_l = \frac{\rho_l u_{rel}^2 r_0}{\sigma} \end{cases} \quad (27)$$

here, T is Taylor Number, respectively. Change of droplet radius has following form in KH model:

$$\frac{dr}{dt} = -\frac{r_0 - r_c}{\tau_{bu}} \quad (28)$$

here, new droplet radius and dimensionless time of the breakup are as follows:

$$r_c = B_0 \cdot \Lambda_{KH} \quad (29)$$

$$\tau_{bu} = 3.788 \cdot B_1 \frac{r_0}{\Lambda_{KH} \cdot \Omega_{KH}} \quad (30)$$

where, B_1 will be determined experimentally. The KH breakup model is valid in case of:

$$B_0 \cdot \Lambda_{KH} \le r_0. \tag{31}$$

Rayleigh–Taylor (RT) instability is another breakup model that is depended on velocity reduction of fuel spray. This model is able to couple with KH model. Schematic of secondary breakup based in KH and RT instabilities are shown in Figure 8.

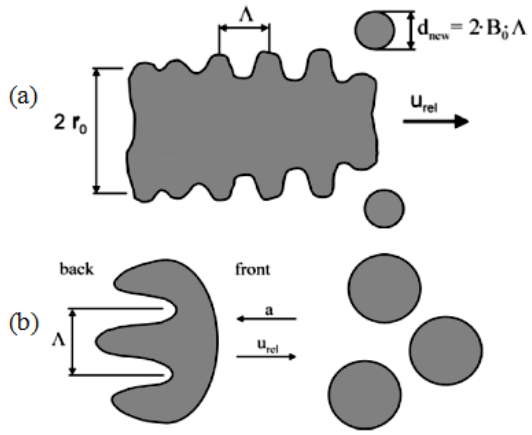

Figure 8. Schematic of secondary breakup based on (a): Kelvin-Helmholtz and (b): Rayleigh-Taylor [44]

In RT model, growth rate of the instability wave (Ω_{RT}) and its corresponding wavelength (Λ_{RT}) are defined by Bellman and Pennington [45] as follows:

$$\Omega_{RT} = \sqrt{\frac{2}{2\sqrt{3\sigma}} \frac{\left[a(\rho_l - \rho_g)\right]^{3/2}}{\rho_l + \rho_g}} \tag{32}$$

$$\Lambda_{RT} = C_3 2\pi \sqrt{\frac{3\sigma}{a(\rho_l + \rho_g)}} \tag{33}$$

where, a as acceleration of the droplet is:

$$a = \frac{3}{8} C_D \frac{\rho_g u_{rel}^2}{\rho_l r}. \tag{34}$$

As one breakup model is unable to simulate the breakup accurately, hybrid breakup models are presented. One of these hybrid models is KH-RT model (See Figure 9), where KH model will be used nearby the injector nozzle and RT will be used in certain distance from the nozzle (See Figure 10).

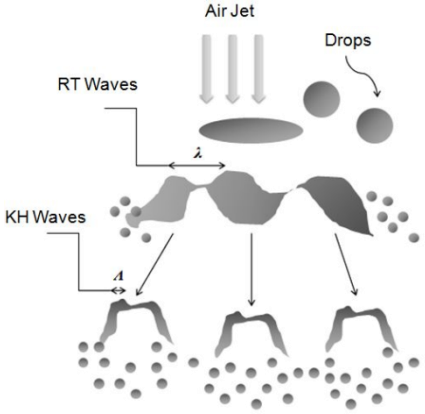

Figure 9. Schematic of KH-RT Breakup model [46]

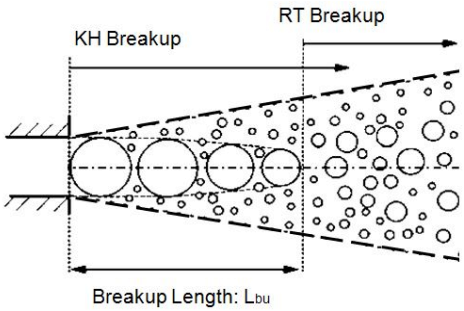

Figure 10. Applying hybrid model of KH-RT

As may be seen in Figure 10, the breakup length (L_{bu}) can be defined as follows:

$$L_{bu} = C \cdot D_{nozzle} \sqrt{\frac{\rho_l}{\rho_g}}. \tag{35}$$

To numerical simulation of fuel spray, different commercial CFD packages such as KIVA, STAR-CCM and AVL FIRE and open source CFD software such as OpenFOAM are introduced and the ability of each other are shown by scholars. The main computational procedure algorithm in these CFD packages indicated in Figure 11.

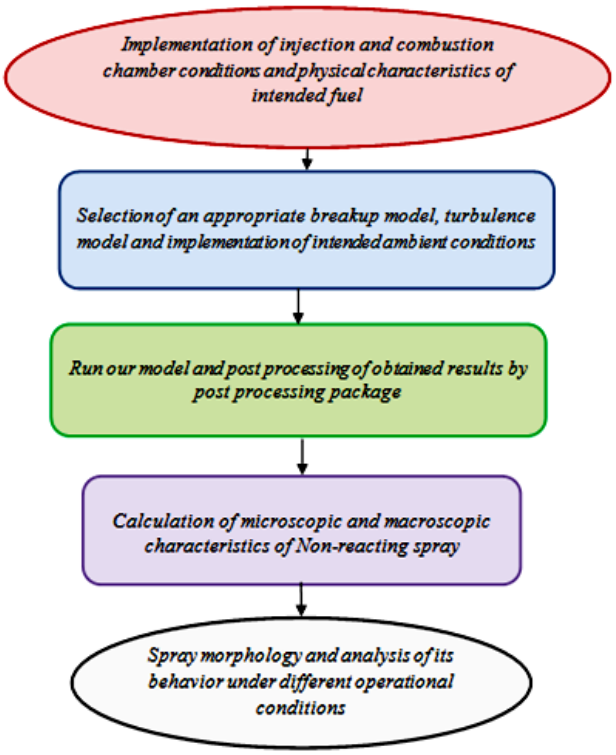

Figure 11. Computational procedure algorithm to study of non-reacting spray

Finally, nowadays, due to complicated behavior of non-reacting spray, several numerical and experimental investigations are in progress under different injection pressure, ambient conditions and for different fuels.

4. Conclusion

Physical characteristics of Non-reacting and non-evaporating fuel spray has significant role on the

reacting condition, air-fuel mixture and efficiency of internal combustion engines such as marine diesel engines (MDEs). So, different numerical and experimental researches are done to understand the behavior and physical morphology of non-reacting spray. For CFD simulation of non-reacting spray, different numerical procedure and physical model are tested that in the current paper, more interested ones are discussed. To this accomplishment, after comprehensive literature review study, the morphology of non-reacting spray is described and the microscopic and macroscopic characteristics of non-reacting spray are defined. Finally, the basic of Eulerian-Lagrangian multiphase and different primary and secondary breakup models are presented and discussed. Assessment of the ability of different Multiscale modeling, for comprehensive investigation of non-reacting fuel spray under different injection and ambient conditions can be considered in future works.

Conflict of Interest

The authors have no competing interests.

References

[1] Nowruzi, H., Ghadimi, P. and Yousefifard, M., "A numerical study of spray characteristics in medium speed engine fueled by different HFO/n-butanol blends", *International Journal of Chemical Engineering*, 2014.

[2] Kumar, S., Cho, J.H., Park, J. and Moon, I., "Advances in diesel-alcohol blends and their effects on the performance and emissions of diesel engines", *Renewable and Sustainable Energy Reviews*, 22, 46-72, 2013.

[3] Miers, S.A., Carlson, R.W., McConnell, S.S., Ng, H.K., Wallner, T. and Esper, J.L., "Drive cycle analysis of butanol/diesel blends in a light-duty vehicle", SAE Technical Paper, No. 2008-01-2381, 2008.

[4] Rakopoulos, D.C., Rakopoulos, C.D., Papagiannakis, R.G. and Kyritsis, D.C., "Combustion heat release analysis of ethanol or n-butanol diesel fuel blends in heavy-duty DI diesel engine", *Fuel*, 90(5), 1855-1867, 2011.

[5] Rakopoulos, D.C., Rakopoulos, C.D., Giakoumis, E.G., Dimaratos, A.M. and Kyritsis, D.C., "Effects of butanol–diesel fuel blends on the performance and emissions of a high-speed DI diesel engine", *Energy Conversion and Management*, 51(10), 1989-1997, 2010.

[6] Rakopoulos, D.C., Rakopoulos, C.D., Hountalas, D.T., Kakaras, E.C., Giakoumis, E.G. and Papagiannakis, R.G., "Investigation of the performance and emissions of bus engine operating on butanol/diesel fuel blends", *Fuel*, 89(10), 2781-2790, 2010.

[7] Doğan, O., "The influence of n-butanol/diesel fuel blends utilization on a small diesel engine performance and emissions", *Fuel*, 90(7), 2467-2472, 2011.

[8] Zhang, Z.H. and Balasubramanian, R., "Influence of butanol–diesel blends on particulate emissions of a non-road diesel engine", *Fuel*, 118, 130-136, 2014.

[9] Tornatore, C., Marchitto, L., Mazzei, A., Valentino, G., Corcione, F.E. and Merola, S.S., "Effect of butanol blend on in-cylinder combustion process. Part 2: Compression ignition engine", *Journal of KONES*, 18, 473-483, 2011.

[10] Biao, D., Zhiyu, H., Zheng, C., Yun, L., Xiaokang, Z. and Guoguang, W., "A study on performance and soot emission of a high-speed diesel engine fueled with butanol-diesel blends", *In Electric Information and Control Engineering (ICEICE)*, 4742-4745, 2011.

[11] Musculus, M.P., Miles, P.C. and Pickett, L.M., "Conceptual models for partially premixed low-temperature diesel combustion", *Progress in Energy and Combustion Science*, 39(2-3), 246-283, 2013.

[12] Nowruzi, H. and Ghadimi, P., "Effect of water-in-heavy fuel oil emulsion on the non-reacting spray characteristics under different ambient conditions and injection pressure: A CFD study", Sci Iran Trans B, 23(6), 2626-2640, 2016.

[13] Ghadimi, P., Nowruzi, H., Yousefifard, M. and Chekab, M.A.F., "A CFD study on spray characteristics of heavy fuel oil-based microalgae biodiesel blends under ultra-high injection pressures", *Meccanica*, 52(1-2), 153-170, 2017.

[14] Ghadimi, P. and Nowruzi, H., "Effects of heavy fuel oil blend with ethanol, n-butanol or methanol bioalcohols on the spray characteristics", *Journal of Applied Fluid Mechanics*, 9, 2016.

[15] Nowruzi, H., Ghadimi, P. and Mirsalim, S.M., "A numerical study on non-reacting spray characteristics of different marine diesel fuel-water emulsion blends", *The Journal of Engine Research*, 44(44), 65-77, 2016.

[16] Nowruzi, H., Ghadimi, P., Yousefifard, M. and Feiz, M.A., "Numerical simulation of non-evaporating and non-reacting heavy fuel oil injection spray in medium speed engines using OpenFOAM", *International Journal of Recent advances in Mechanical Engineering*, 3(2), 2014.

[17] Nowruzi, H., Ghadimi, P. and Yousefifard, M., "Large eddy simulation of ultra-high injection pressure diesel spray in marine diesel engines", *Transactions of FAMENA*, 38(4), 65-76, 2015.

[18] Yousefifard, M., Ghadimi, P. and Nowruzi, H., "Three-dimensional LES modeling of induced gas motion under the influence of injection pressure and ambient density in an ultrahigh-pressure diesel injector", *Journal of the Brazilian Society of Mechanical Sciences and Engineering*, 37(4), 1235-1243, 2015.

[19] Ghadimi, P., Yousefifard, M. and Nowruzi, H., "Particle and gas flow modeling of wall-impinging diesel spray under ultra-high fuel injection pressures", *Journal of Applied Fluid Mechanics*, 10(5), 2017.

[20] Nishida, K., Zhang, W. and Manabe, T., "Effects of micro-hole and ultra-high injection pressure on mixture properties of DI diesel spray", SAE Transactions, 421-429, 2007.

[21] Wang, X., Huang, Z., Kuti, O.A., Zhang, W. and Nishida, K., "Experimental and analytical study on biodiesel and diesel spray characteristics under ultra-high injection pressure", *International journal of heat and fluid flow*, 31(4), 659-666, 2010.

[22] Ghasemi, A., Barron, R.M. and Balachandar, R., "Spray-induced air motion in single and twin ultra-high injection diesel sprays", *Fuel*, 121, 284-297, 2014.

[23] Fink, C., Buchholz, B., Niendorf, M. and Harndorf, H., "Injection spray analyses from medium speed engines using marine fuels", *In Proceedings of the 22nd European Conference on Liquid Atomization and Spray Systems (ILASS'08)*, 2008.

[24] Chen, X., Liu, Y. and Yang, V., "Effect of Backpressure on Internal Flow Dynamics and Spray Characteristics of Liquid Swirl Injector", *In 49th AIAA Aerospace Sciences Meeting including the New Horizons Forum and Aerospace Exposition*, 98, 2011.

[25] Park, S.H., Kim, H.J. and Lee, C.S., "Comparison of experimental and predicted atomization characteristics of high-pressure diesel spray under various fuel and ambient temperature", *Journal of mechanical science and technology*, 24(7), 1491-1499, 2010.

[26] Roisman, I.V., Araneo, L. and Tropea, C., "Effect of ambient pressure on penetration of a diesel spray", *International journal of multiphase flow*, 33(8), 904-920, 2007.

[27] Yousefifard, M., Ghadimi, P. and Nowruzi, H., "Numerical investigation of the effects of chamber backpressure on HFO spray characteristics", *International Journal of Automotive Technology*, 16(2), 339-349, 2015.

[28] Ghadimi, P., Yousefifard, M. and Nowruzi, H., "Applying different strategies within OpenFOAM to investigate the effects of breakup and collision model on the spray and in-cylinder gas mixture attribute", *Journal of Applied Fluid Mechanics*, 9(6), 2016.

[29] Najafi, A., Nowruzi, H. and Ghassemi, H., "Performance prediction of hydrofoil-supported catamarans using experiment and ANNs", *Applied Ocean Research*, 75, 66-84, 2018.

[30] Shora, M.M., Ghassemi, H. and Nowruzi, H., "Using computational fluid dynamic and artificial neural networks to predict the performance and cavitation volume of a propeller under different geometrical and physical characteristics", *Journal of Marine Engineering & Technology*, 17(2), 59-84, 2018.

[31] Nowruzi, H., Ghassemi, H. and Ghiasi, M., "Performance predicting of 2D and 3D submerged hydrofoils using CFD and ANNs", *Journal of Marine Science and Technology*, 22(4), 710-733, 2017.

[32] Nowruzi, H., Ghassemi, H., Amini, E. and Sohrabi-asl, I., "Prediction of impinging spray penetration and cone angle under different injection and ambient conditions by means of CFD and ANNs", *Journal of the Brazilian Society of Mechanical Sciences and Engineering*, 39(10), 3863-3880, 2017.

[33] Shinjo, J., Xia, J. and Umemura, A., "Droplet/ligament modulation of local small-scale turbulence and scalar mixing in a dense fuel spray", *Proceedings of the Combustion Institute*, 35(2), 1595-1602, 2015.

[34] Nowruzi, H., Phenomenology of Non-Reacting Spray, LAP LAMBERT Academic Publishing, Germany, 2016..

[35] Jiang, X., Siamas, G.A., Jagus, K. and Karayiannis, T.G., "Physical modelling and advanced simulations of gas–liquid two-phase jet flows in atomization and sprays", *Progress in energy and combustion science*, 36(2), 131-167, 2010.

[36] Naber, J.D. and Siebers, D.L., "Effects of Gas Density and Vaporization on Penetration and Dispersion of Diesel Sprays", SAE Technical Report, 1996.

[37] Blazek, J., Computational Fluid Dynamics: Principles And Applications, Butterworth-Heinemann, 2015.

[38] Raudkivi, A.J. and Callander, R.A., Advanced Fluid Mechanics: An Introduction, New York, Halsted Press, 1975.

[39] Launder, B.E. and Spalding, D.B., Mathematical Models of Turbulence, Academic press, 1972.

[40] Ferziger, J.H. and Peric, M. Computational Methods for Fluid Dynamics, Springer, New York, 2002.

[41] Reitz, R.D., Diwakar J, "Effect of drop break-up on fuel sprays," SAE Technical Paper No.860469, 1986.

[42] Reitz, R.D., Diwakar R, "Structure of high-pressure fuel sprays", SAE Technical Paper, No.870598, 1987.

[43] Reitz, R.D., "Modeling atomization processes in high pressure vaporizing sprays", *Atomization Spray Technol*, 3,309-37, 1987.

[44] Baumgarten, C., Mixture Formation in Internal Combustion Engine, Springer, New York, 2006.

[45] Bellman, R., Pennington, R., "Effects of surface tension and viscosity on Taylor instability", *Q Appl Math*, 12,151-162, 1954.

[46] Hossainpour S, Binesh AR., "Investigation of fuel spray atomization in a DI heavy-duty diesel engine and comparison of various spray breakup models", *Fuel*, 88, 799-805, 2009.